Available online at www.sciencedirect.com
SCIENCE DIRECT®
C. R. Physique 4 (2003) 465–474
COMPTES RENDUS PHYSIQUE

Exotic nuclei/Les noyaux exotiques

Covalently bound molecular states in beryllium and carbon isotopes

Wolfram von Oertzen [a,b], Hans-Gerhard Bohlen [a]

[a] *Hahn-Meitner-Institut, Glienicker Str. 100, 14109 Berlin, Germany*
[b] *Fachbereich Physik, Freie Universität Berlin, Germany*

Presented by Guy Laval

Abstract

Nuclear clustering in $N = Z$ nuclei has been studied since many decades. States close to the decay thresholds, as described by the Ikeda diagram, are of particular interest. Recent studies in loosely bound systems, as observed with neutron-rich nuclei has revived the interest in cluster structures in nuclei, with additional valence neutrons, which give rise to pronounced covalent molecular structures. The Beryllium isotopes represent the first example of such unique states in nuclear physics with extreme deformations. In the deformed shell model these are referred to as super- and hyper-deformation. These states can be described explicitly by molecular concepts, with neutrons in covalent binding orbits. Examples of recent experiments performed at the HMI-Berlin demonstrating the molecular structure of the rotational bands in Beryllium isotopes are presented. Further work on chain states (nuclear polymers) in the carbon isotopes is in progress, these are the first examples of deformed structures in nuclei with an axis ratio of 3 : 1. A threshold diagram with clusters bound via neutrons in covalent molecular configurations can be established, which can serve as a guideline for future work. ***To cite this article: W. von Oertzen, H.-G. Bohlen, C. R. Physique 4 (2003).***

Résumé

Liaison covalente des états moléculaires dans les isotopes de Béryllium et de Carbone. L'apparission d'agrégats dans les noyaux $N = Z$ est discutée depuis longtemps. Les états dont l'énergie est proche de l'ouverture d'un canal de décroissance en fragments, comme le décrit le diagramme d'Ikeda sont particulièrement interessants. Les études récentes sur les noyaux faiblement liés, riches en neutrons par exemple, a remis au goût du jour les agrégats dans les noyaux avec un phénomène nouveau : l'apparition de structures moléculaires covalentes stabilisées par la présence de neutrons de valence. Les isotopes de Béryllium représentent le premier exemple de tel états avec une déformation extrême en physique nucléaire. Dans le cadre du modèle en couche déformé ces états correspondent aux états super- ou même hyper-deformés. Des exemples d'expériences récentes faites au HMI de Berlin montrent la structure moléculaire des bandes rotationnelles des isotopes de Béryllium. D'autres travaux cherchant à mêttre en évidence des polymères nucléaires dans les isotopes de Carbone (des chaînes d'α) sont en cours, ce serait la première observation de noyaux hyper déformés, i.e. des élipsoides allongé possédant un rapport d'axe de 3 : 1. Un diagramme présentant les seuils de fragmentation des agrégats liés par des neutrons de valence est proposé pour guider les travaux futurs. ***Pour citer cet article : W. von Oertzen, H.-G. Bohlen, C. R. Physique 4 (2003).***

Keywords: Neutron rich nuclei; Nuclear clusters and molecules

Mots-clés : Noyaux riches en neutrons ; Agrégats des neutrons et molécules

E-mail addresses: oertzen@hmi.de (W. von Oertzen), bohlen@hmi.de (H.-G. Bohlen).

1631-0705/03/$ – see front matter
doi:10.1016/S1631-0705(03)00052-5

1. Clusters, molecular potentials and nuclear molecules

The concept of clustering in nuclei has a 40 year old background, or an even older one if early models of the nucleus are considered, before the discovery of the neutron [1]. Clustering phenomena in nuclei, related to alpha-particle or heavier closed shell clusters, have been predicted from different models, such as the cranked α-cluster models [2,3], from Hartree–Fock calculations [4], from Nilsson–Strutinsky calculations [5] and others [6]. The experimental tools for the observation of cluster structures in $N = Z$ nuclei has been the domain of charged particle spectroscopy. Various decay studies for the spectroscopy of strongly deformed shapes in $N = Z$ nuclei with the emission of α-particles, of ^{8}Be and heavier fragments are known [7–9]. Recently new studies with detector set-ups combining particle and γ detection are expected to give new insight into exotic shapes in nuclei related to clustering.

The advances in the study of neutron-rich light nuclei has attracted worldwide attention, because the weakly bound nuclear systems exhibit unique features related to the quantal properties of the many body systems; in particular let us mention the clustering and halos (see contributions to this volume). It turned out that the structure of states of the beryllium isotopes is a very special starting point for the discussion of clustering phenomena in neutron-rich light nuclei, where the additional valence neutrons are in configurations, which are rather independent from the mean field concepts of nuclear structure and give rise to covalently bound structures in nuclear physics [10].

1.1. The local α–α potential, threshold diagrams

The formation of molecular structures, in particular in beryllium isotopes, relies on special properties of the potentials between the cluster cores, namely the occurrence of a 'molecular' potential. For the real part of the potential we should have attraction at large distances and repulsion at small distances. This property of the cluster–cluster interactions must be also considered as the origin of the Ikeda diagram [11,12]. In addition the absorption (or spreading width) of the cluster penetrating the nuclear medium (the other nucleus) determines the amplitude to observe the cluster in the nuclear medium. A high chemical potential (separation energy) for nucleons in the cluster will give the cluster a long life time, that is a small absorption as in the case of α-particles, or in $^{16}\mathrm{O} + {}^{16}\mathrm{O}$ scattering, where pronounced rainbow maxima are observed [13,14]. For the description of molecular states the local potentials, which are usually shallow, have to be considered. An example is the potential by Ali and Bodmer for the α–α-potential [15]. Such potentials are obtained by 'supersymmetric' transformations as discussed by Baye [16]. We have two quite conspicuous cases, where the local potentials have a small attractive part and a strong repulsion at small distances, and the absorption is generally rather weak; these cases are α-particles interacting with α-particles and with ^{16}O, see also [17,18]. The repulsion at small distances originates from the Pauli blocking, in the case of the $\alpha + \alpha$ potential the nucleons of the second cluster have to move up into the next major shell. These potentials, which are repulsive at small distances are needed in order to build *covalently bound nuclear cluster structures* for nuclei with additional neutrons as discussed in the next section.

Neutron-rich and weakly bound nuclei show a strong tendency to clustering [9,10,19–21]. Model independent calculations based on the method of antisymmetrised molecular dynamics indicate [20–23], that clustering in weakly bound and in neutron rich nuclei is also favoured by a mean field effect, where due to certain properties of the nuclear forces the interactions can saturate better in a larger volume by forming several clusters with $N = Z$. In this way for the surplus valence neutrons due to the larger deformation and surface a maximum number of protons can be shared by the neutrons. However, additional quantal effects related to concepts of molecular physics, and due to the strong clusterization these states in nuclei lead further to the formation of shape isomers in the form of covalent molecular structures.

1.2. Nuclear deformation and the correlation diagram

We can discuss the occurrence of particular shapes in light nuclei and deformations related to clusters by inspection of the deformed harmonic oscillator diagram shown in Fig. 1 (adopted from [24] and [25]). Stable oblate and prolate shapes are expected for particular (magic) numbers (N) of nucleons, which are referred to as deformed shells. This level diagram indicates that deformed shapes with stable configurations (for large energy gaps) are expected for positive values of the deformation parameter, $\beta_2 > 0$, and special ratios of the two main axes, namely 2 : 1 (the dimers in berylium isotopes) and 3 : 1 (chain states in carbon isotopes) and even longer chains. For $\beta < 0$ and $N = 6$ (carbon), we have an oblate deformed shell with the axes ratio 1 : 2. This can give rise to triangular shapes [25]. Thus for ^{12}C, as well as for ^{13}C and ^{14}C and in ^{28}Si, the coexistence of oblate and prolate deformed states is predicted. The degeneracy in the orbits shown in the diagram of Fig. 1 is given by the occupation with nucleons (black dots in the diagram), it is 2 for the lowest projection (n_z) and rises to 4 and 6 for the higher orbits.

Having well defined clusters, we will apply the molecular orbital model for nucleons in the same way as in atomic physics via the linear combination of nuclear orbitals (LCNO [26,27]). The molecular orbital model for neutrons has been applied extensively to nuclear collisions involving single neutron transfer [26–31]. This can be done for low energies, and for cases

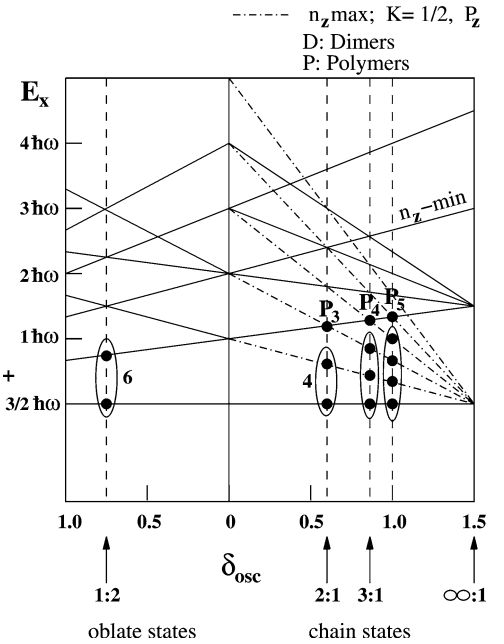

Fig. 1. Diagram of shells in a deformed harmonic oscillator potential for axially symmetric shapes; some 'magic' numbers of nucleons for prolate configurations related to dimers and to chain states are emphasized. The orbits are split due to the values of the relevant quantum numbers, K – projection of angular momentum, and n_z – number of nodes on the z-axis. The $K = 1/2$ orbits give rise to deformed shells with particular degeneracies (P_z), with the formation of chain states. The energy is counted from the lowest level ($3/2\hbar$) plus additional units of harmonic oscillator quanta. Oblate ($\delta < 0$) and prolate ($\delta > 0$) quadrupole deformations occur. The parameter δ_{osc} in the figure is given in terms of the deformed oscillator frequencies ω_i: δ_{osc} is defined as: $\delta_{\text{osc}} = 3(\omega_p - \omega_3)/(2\omega_p + \omega_3)$ (adopted from [24]).

where strongly bound cores (typically alpha-cluster nuclei) and valence nucleons are defined in a clear way [30]. In a collision process this approach corresponds to a choice of two-centre basis states and the couplings appear as radial and Coriolis couplings [27,29]. This approach must be considered as an equivalent approach to the coupled reaction channel calculations based on the asymptotic basis states of the separated nuclei [32]. A comparison of the two approaches can be found in [31]. The original studies based on the LCNO model [26–28,33] were limited to scattering states for two heavier nuclei, where the core-core optical potential usually becomes strongly attractive and absorptive, once the Coulomb barrier is reached. However, new insights into the properties of cluster-cluster interaction may necessitate a reappraisal of these studies.

In the two-centre shell model not only valence nucleons, but all nucleons are considered, and a correlation diagram as in Fig. 2, has to be calculated [26,34]. Such correlation diagrams of molecular configurations are well known in atomic physics (see also [35], p. 328). The molecular orbits merge at small distances with the Nilsson-orbits of the deformed compound nucleus. The molecular orbitals are classified according to the well known quantum numbers of molecular valence states: the K-quantum number for the projection of the spin, and the σ and π orbitals stand for the $M = 0$, and $M = 1$ projections of the orbital angular momenta l. In addition to the parity, the *gerade* (g) and *ungerade* (u) symmetry appears for the case of the identity of the two molecular cores.

With this correlation diagram we are able to discuss the structure of the isotopes ^{9}Be, ^{10}Be and ^{11}Be, if we consider [10] the population of the molecular orbitals for a distance corresponding to the minimum in the α–α potential, or in the Nilsson model, to a deformation of $\beta_2 = 0.6$–0.7, see Fig. 2.

In the Ikeda diagram [11,12] for $N = Z$ nuclei clustering in nuclei becomes relevant for states close to their thresholds for the decomposition into clusters. We extend this diagram by adding neutrons and considering loosely bound states. We expect to observe molecular structures based on clusters, which are bound by covalent neutrons at energies in the vicinity of (or also well below) the corresponding thresholds. Using a cluster plus valence neutrons model the extension of this concept was formulated in [10]. The covalent binding of neutrons produces a new diagram as shown in Fig. 9, the 'Covalent Molecular Binding Diagram': *covalently bound molecular structures will appear in neutron rich nuclei close to the thresholds for decomposition into neutrons, α-clusters, and other clusters*. For reasons of simplicity, in Fig. 9 only the combinations of alpha-clusters and spherical clusters (^{16}O) are considered, because with deformed clusters more complicated spectra will appear. For the asymmetric molecules rotational bands as parity doublets are observed [18,52].

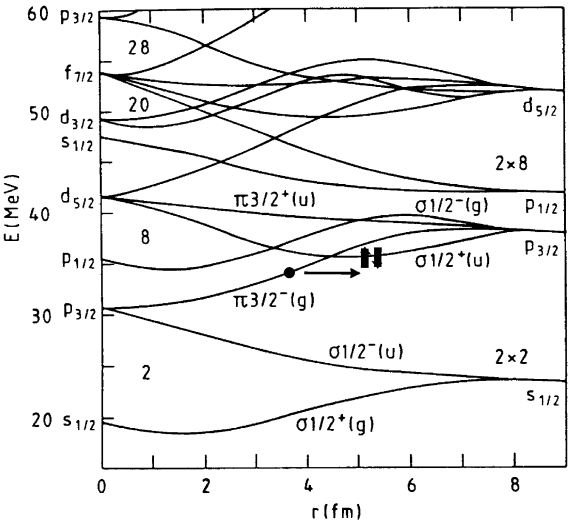

Fig. 2. Correlation diagram of molecular orbitals in a two-centre shell model picture; the molecular orbitals are labelled by their quantum numbers (see text). The distance between the two centres is denoted by r. The minimum of the $\alpha-\alpha$ potential occurs for the ground state of ^{9}Be at a distance of about 3.3 fm, and the structure of excited states in $^{9-11}$Be is determined by $\alpha-\alpha$ distances of $r = 2.7$–5 fm. The largest distances are reached for molecular rotational bands, e.g., the $K = 3/2^{-}$ band in ^{11}Be, which is populated by adding two neutrons to ^{9}Be in the $(\sigma)^2$-configuration, the $\alpha-\alpha$ distance increases in that case as indicated.

As the basic building block of such covalently bound nuclear molecules we will discuss in the following the case of the Beryllium isotopes. The case of more extended molecules based on the combinations of α-particles and ^{16}O-clusters is discussed in [18].

2. Dimers, the beryllium isotopes

The first deformed structure in nuclear physics with an axis ratio of 2 : 1 is the unbound (by 92 keV) ^{8}Be-nucleus, consisting of two α-particles in an $L = 0$ resonant state. It can thus be regarded as a superdeformed nucleus. Further it has been known for more than two decades, that the ground state of the ^{9}Be nucleus can be explained by a covalent molecular binding, where two α-particles are bound by the $p_{3/2}$ valence neutron. The projection of the nucleon spin on the symmetry axis (as in the Nilsson model) can have two values $K = 3/2$, and $K = 1/2$. In the framework of molecular orbitals the first corresponds to π, the latter to a σ molecular orbital which merge into the Nilsson orbitals at smaller distances.

The level structure of $^{9-12}$Be has been established with a variety of light ion induced single and multi-nucleon transfer reactions. These results have been compiled under the aspect of covalent molecular binding and the corresponding rotational bands where identified in 1996/97 by von Oertzen [10]. This was met with great scepticism, although 'unnoticed' in the literature the method of molecular orbitals has been applied quite successfully and also to ^{10}Be (see references cited in [10]).

Inspecting the correlation diagram and starting from large distances with the splitting of the molecular orbitals, we note (see Fig. 2), that close to the minimum of the α–α potential the $K = 3/2^{-}$–π-orbit crosses the $K = 1/2^{+}$–σ-orbit and becomes the lowest state at smaller distances. The sequence of excited levels of ^{9}Be, and also in ^{10}Be for two valence particles, can thus completely be explained as rotational excitations of the basis states obtained by this scheme. Two points are very remarkable in this observation, see Figs. 3 and 6: (i) large moments of inertia of the excited bands in ^{10}Be ($K = 0_2^{+}$ and 1^{-}) and ^{11}Be ($K = 3/2^{-}$), both are related to the occupation of the σ-orbit with neutrons; (ii) the very pronounced Coriolis decoupling pattern for the $K = 1/2^{+}$ band in ^{9}Be (also observed with the same strength for the $K = 1/2$ band in ^{11}Be, see [10]), characteristic for a strongly deformed molecular structure with two centers. Microscopic cluster calculations of Descouvemont for ^{9}Be using the Generator Coordinate method reproduce perfectly this decoupling effect [40].

In our systematic study of the structure of beryllium isotopes [10,39] rotational bands of ^{9}Be, ^{10}Be, ^{11}Be and ^{12}Be could be identified, which show a very large distance between the two α-clusters and can therefore be characterized as molecular structures. For ^{10}Be, ^{11}Be and ^{12}Be an α–α distance of about 5 fm is deduced from the moment-of-inertia Θ obtained from a fit of excitation energies versus $J(J+1)$, where J is the spin in the corresponding state: $E_x(J) = E_{x,K} + \hbar^2/(2\Theta)\ [J(J+1) - K(K+1)]$. According to the correlation diagram of Fig. 2, the structure of these states is

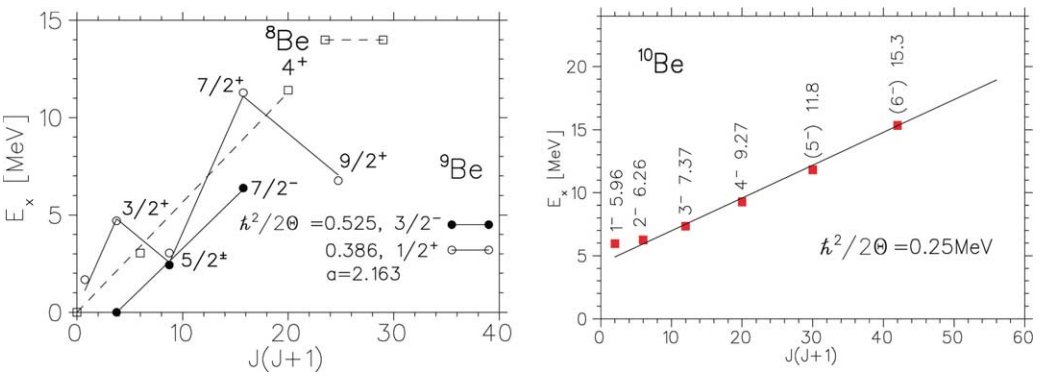

Fig. 3. Rotational bands of ^{8}Be, ^{9}Be (left panel) and ^{10}Be (right panel) plotted as function of angular momentum $J(J+1)$. The Coriolis decoupling parameter, a, for the $K = 1/2$ band is indicated. The experimental values of excitation energies are from [36–39].

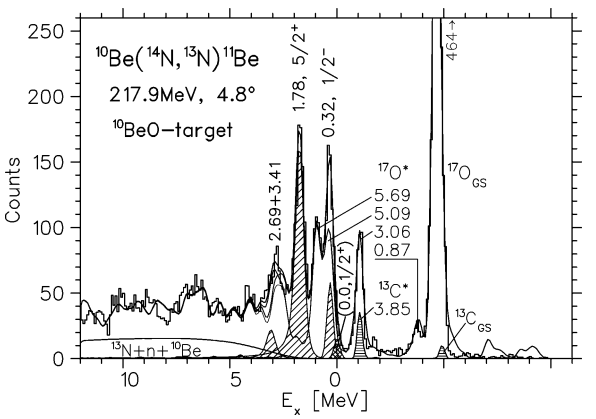

Fig. 4. Excitation of states in ^{11}Be in the *one-neutron transfer* on ^{10}Be, note the absence of the states of the $K = 3/2^-$ band, observed very prominently in Figs. 5 and 6.

determined by the evolution of the π and σ orbitals as functions of the distance. The ground state of ^{10}Be can be interpreted as a $(\pi)^2$ configuration, whereas the excited 0_2^+ at 6.179 MeV in ^{10}Be is interpreted as the $(\sigma)^2$ configuration, which attains its energy minimum at larger core-core distances. With two neutrons in a π-orbit the slope of these orbits favours a smaller distance between the two cores. The ground states of ^{10}Be and ^{12}Be have therefore a much more compact shape. For ^{12}Be larger moments of inertia are again expected for excited bands, when $(\sigma)^2$ configurations are involved (see also the contribution by Freer to this volume [41]).

3. Experimental results on the structure of $^{10–12}$Be

Because of the distinct differences in the structure of states in the beryllium isotopes, the population of states via one-neutron or two-neutron transfer based on different target wave functions can give very complementary results. Very remarkable is the $K = 3/2^-$ band [10] in ^{11}Be, which starts at 3.96 MeV, with states established to high excitation energies [43–45]. In contrast to this the one neutron transfer on a ^{10}Be-target populates only very few states (Fig. 4), all of single-particle character, due to the compact $(\pi)^2$ configuration of the ^{10}Be ground state. The isomeric molecular states of the $K = 3/2^-$ band in ^{11}Be are only populated in $2n$-transfer reactions on ^{9}Be, as shown in Figs. 5 and 6. In fact, these narrow high-lying states (the $1n$-threshold is at 0.5 MeV) where already observed in the (t, p) reaction by Ajzenberg-Selove [42] up to 10.7 MeV, which corresponds to a state with $J^\pi = 11/2^-$ in our tentative assignment. The band head is neutron-unstable by 3.46 MeV but has a width of only 15(5) keV [42]. These states are interpreted as based on the $(\pi)^1 \times (\sigma)^2$ configuration. Very remarkable is the extension of the rotational band to the potentially highest values of angular momentum. With two valence particles in the $1d_{5/2}$ shell and one particle in the $1p_{3/2}$ shell, the maximum single particle angular momentum is $11/2$. Adding the angular momentum of the core-core relative motion of the two α-particles (with the possible values of 2 and 4), we can indeed reach $19/2$ as a maximum

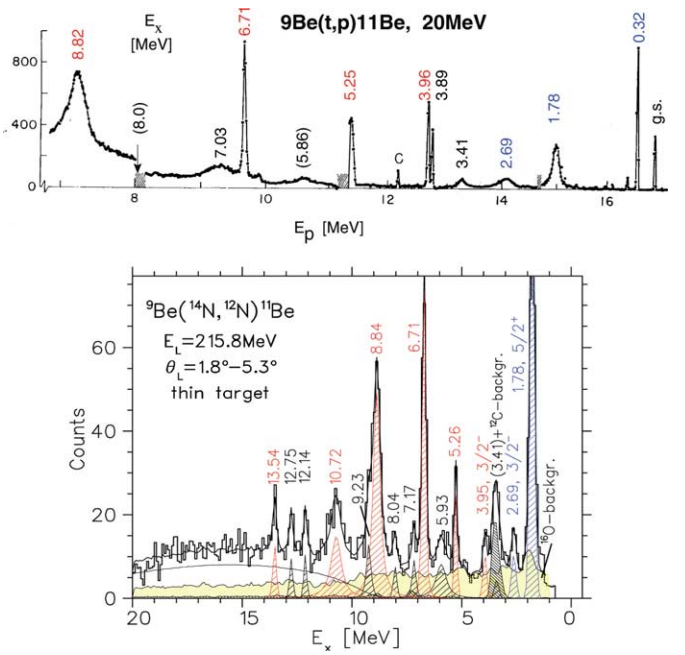

Fig. 5. Population of states in ^{11}Be in *two-neutron transfer* reactions on ^{9}Be: upper panel ^{9}Be(t,p) [42], lower panel: ^{9}Be(^{14}N,^{12}N) [39] (see also Fig. 6). Note the rather small widths of states of the $K = 3/2^-$ band starting at 3.95 MeV (these states are marked in red), well above the neutron threshold of 0.5 MeV.

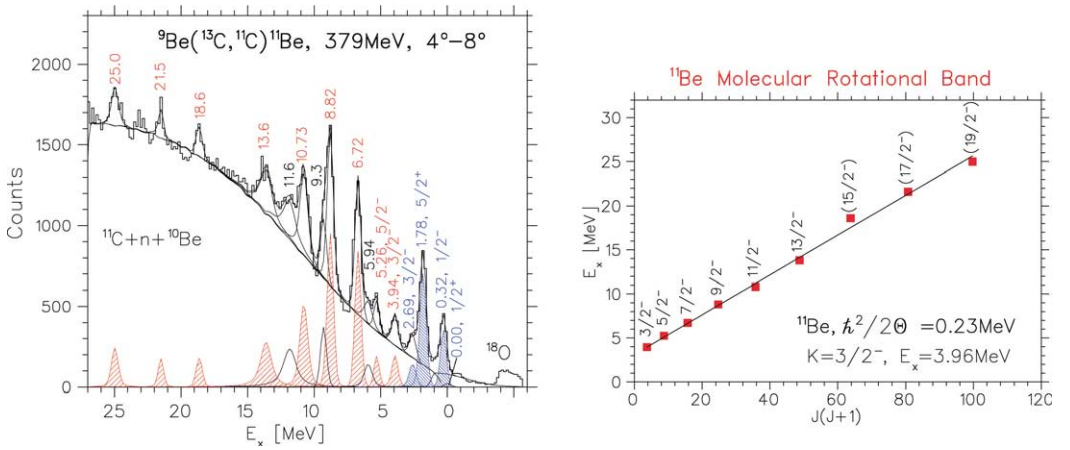

Fig. 6. Left panel: Spectrum of the ^{9}Be(^{13}C,^{11}C) reaction measured at high incident energy. Members of the $K = 3/2^-$ band are marked in red. Right panel: Excitation energies of states of the $K = 3/2^-$ band plotted as function of $J(J + 1)$ (the higher lying states are tentatively assigned).

spin value. With the slope parameter of 0.23 MeV (see Fig. 6) the moment-of-inertia of the $K = 3/2^-$ band is very similar to that of the excited $K = 1^-$ band in ^{10}Be (Fig. 4). Note that the deformed shell model has difficulties to explain the highest spins.

The proposed molecular properties of the states in Be-isotopes have found striking confirmation from 'model independent' calculations by Kanada-En'yo and Horiuchi [20,21,23] using the method of Antisymmetrised Molecular Dynamics (AMD), and partially also from cluster model calculations by Descouvemont and Baye [40,46,47]. Particularly impressive are the density distributions in the AMD calculations with their characteristic differences, obtained for the ground state 0_1^+ and second 0_2^+ state of ^{10}Be, as well as the recently published nucleon densities for the $K = 3/2^-$ band in ^{11}Be [23]. The formation of covalent bonds with the $(\sigma)^2$ for the second 0_2^+ and for the $(\pi)^2$-configurations is very conspicuous in the density distributions obtained

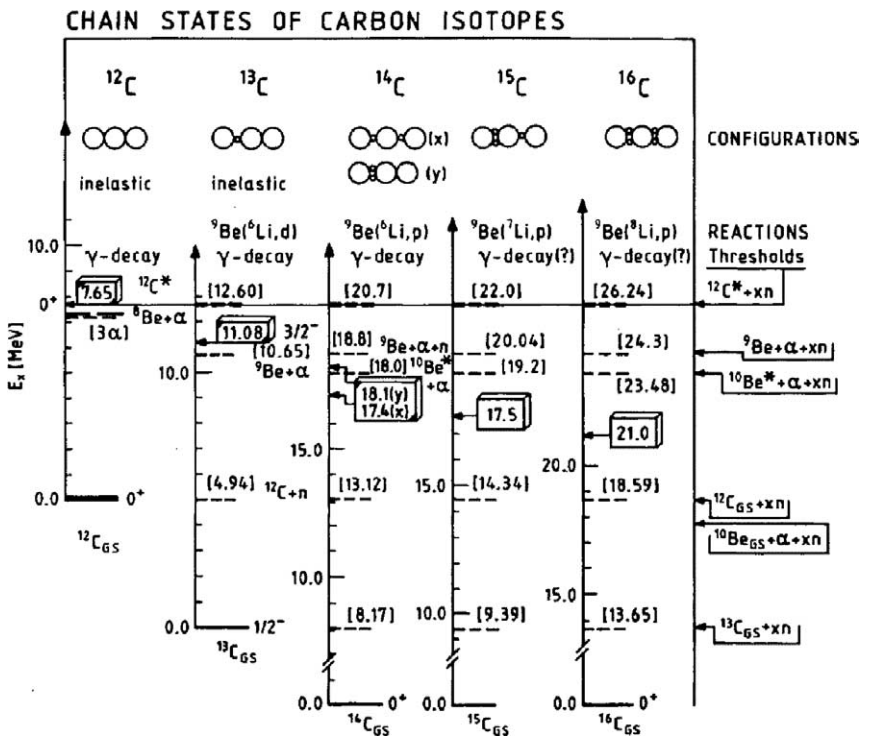

Fig. 7. Proposed chain states of carbon isotopes [10] with up to four extra covalent valence neutrons. The thresholds for the decay into α-particles and neutrons are aligned to the same level, and other thresholds are shown. The boxes indicate the energies, where covalently bound structures are expected to appear.

from these calculations [21], in complete agreement with expectations from the correlation diagram in Fig. 2. The most recent result of the AMD method [23] for the states in ^{11}Be again give a striking confirmation of the dimer structure for both, the $K = 1/2$ and in particular for the $K = 3/2^-$ band, where the density distributions show two well separated alpha-particles. The $K = 3/2^-$ band is obtained in the AMD calculations with seven band members [23].

The molecular structure is still visible in heavier isotopes of Be, such as ^{12}Be, where the persistence of the strong clustering of the α-particles prevents the formation of a closed shell with $N = 8$, for which a spherical nucleus would be expected. In 1999 two molecular rotational bands have been identified in ^{12}Be using different experimental techniques: (i) the fragmentation of ^{12}Be into two ^{6}He particles, which were detected using an angular correlation setup [48]; and (ii) the transfer of three neutrons to ^{9}Be in the reaction ^{9}Be(^{15}N,^{12}N)^{12}Be, where also states up to 22 MeV excitation energy were observed [44]. AMD calculations for ^{12}Be have been successfully performed by Kanada-En'yo [49]. We turn now to recent results obtained concerning the chain states in the carbon isotopes.

4. Polymers, chain states in carbon isotopes

Similar to the covalently bound structures of two α-particles and neutrons discussed above, linear chain states with *three α-particles* can be constructed, which have extreme deformations with an axes ratio of 3 : 1. These *trimers* are built by covalent binding extrapolating from the well established knowledge of the covalent bonds in ^{9,10}Be. We may expect that covalently bound linear chain isomers in $^{13-16}$C are formed close to or rather well below the relevant three-α + neutrons thresholds. The two bonds in the covalent configuration between the three α-particles will influence each other so as to increase the total binding energy of the chain. This can be formulated by starting with a ^{9}Be + α basis, or with a three center molecular orbital approach, see [52]. Explicit molecular orbit calculations for ^{14}C and ^{16}C are discussed by Itagaki in [50,51].

We now have a short look into the properties of ^{13}C, for which the experimental evidence has recently been compiled [52]. The structure of the linear chain configurations for ^{13}C (and ^{14}C), when based on the α + ^{9}Be (or α + ^{10}Be) structure corresponds to an intrinsic reflection asymmetric configuration, similar to the well known cases in ^{20,21}Ne nuclei [13]. This

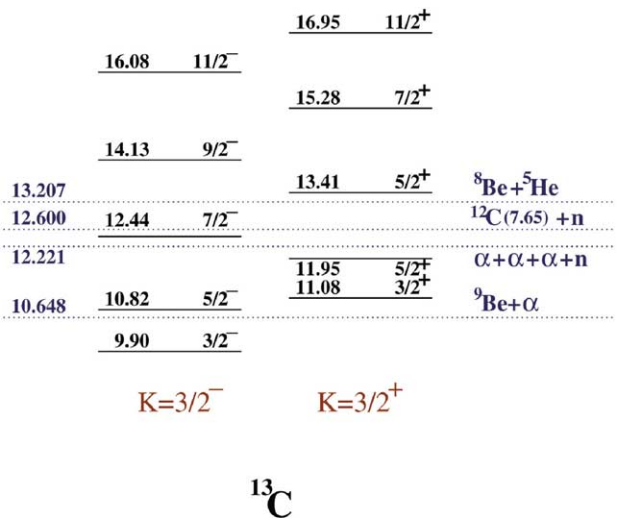

Fig. 8. Proposed rotational α-cluster bands in ^{13}C [52]. These are states which cannot be attributed to single particle states based on ^{12}C (g.s., 2_1^+ and 1_1^+), their energies plotted as function of their spins, $J(J+1)$, form two rotational bands, a parity split inversion doublet with K-quantum number $3/2$. Various thresholds are indicated by dotted lines.

Table 1
Moments of inertia of molecular rotational bands corresponding to strongly deformed configurations in nuclei with $A = 10$–16

Nucleus	Band head: K^π, E_x [MeV]	$\hbar^2/2\Theta$ (keV)	References
^{10}Be	0_2^+, 6.179; 1_1^-, 5.960	250	[10,39]
^{11}Be	$3/2^-$, 3.96	230	[43,45]
^{12}Be	0^+ (6.4); 0^+ (10.8)	210; 150	[44]; [48]
^{13}C	$3/2_2^-$, 9.90; $3/2_3^+$, 11.08	190	[52]
^{16}C	0^+ (>22)	150	predicted in [51]

has the consequence that inversion parity doublets must be observed with the K-quantum number $K = 3/2^{-,+}$ for the ^{9}Be–α structure.

In order to establish such structure an attempt has been made recently for a complete spectroscopy in ^{13}C [52]; all the states related to single particle structure are first removed, than the remaining states were carefully scrutinized for their spectroscopic properties such as their population in different multi-nucleon transfer reactions, in particular α-capture reactions. The result shows two rotational bands as partners of a parity doublet; these are shown in Fig. 8. Considerations using the Hueckel Method for three-center (linear) molecules [52] give also a good description of the observed structures, in particular the position of the band heads relative to the $\alpha + {}^9$Be threshold. These two bands are thus the first examples of really hyperdeformed (axis ratio 3 : 1) nuclear structures in nuclei.

A publication with the systematic study of known levels in ^{14}C and with results from new recent experiments is in preparation [53].

5. Conclusions

To conclude the results of these considerations, we can state that there is strong evidence for states in light nuclei with strong clustering based on alpha-particles and covalently bound neutrons, which are observed as dimers in Beryllium isotopes, and trimers in $^{13-16}$C.

We summarize in Table 1 the moments of inertia of the rotational bands determined in recent work for these isomeric molecular states in light nuclei. We note that the large moments of inertia observed in the Be-isotopes are surpassed by the value found for the ^{13}C bands. The latter states can be considered as even more deformed (hyperdeformed) configurations, which are due to clustering and binding due to covalent molecular orbits of the valence neutrons.

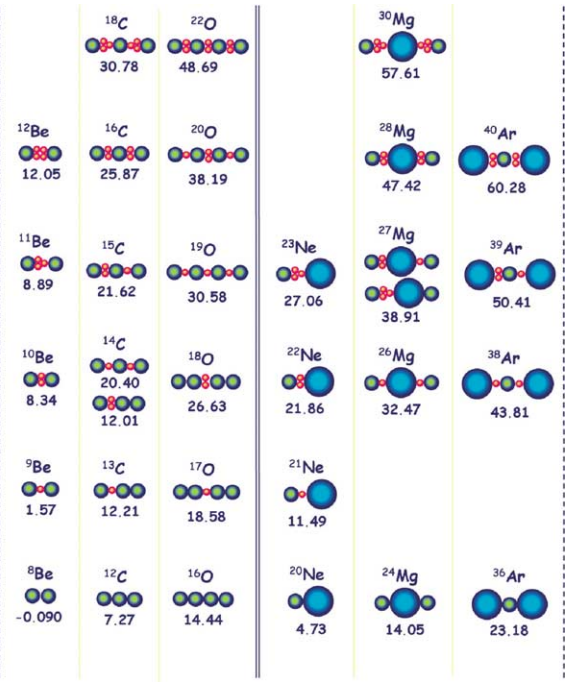

Fig. 9. The extended threshold diagram of clusters and covalently bound nuclear molecules with valence neutrons. The threshold energies are indicated.

There are also systems with larger clusters forming asymmetric molecules based on α-particles and heavier clusters. The first steps to establish the structure of covalently bound states in nuclear system have now been made [18].

In accordance with these findings it is possible to make a new threshold-diagram for covalently bound nuclear molecular states, as shown in Fig. 9, where the existence of even more extended molecules can be predicted. The configurations which are schematically shown in this figure go beyond the deformed shell model approach, they are true shape isomers, with complicated deformations, which can *not* be easily described by a few terms in the Legendre-function expansions for nuclear shapes. This statement holds already for the observed rotational bands of the molecular structures in the beryllium and carbon isotopes.

Acknowledgement

This work contains results obtained from experiments performed at the ISL facility at HMI-Berlin over the last 10 years. We acknowledge the the work of many students and scientific guests for their major contributions. We thank the funding agencies (DAAD, A.v. Humboldt Stiftung, Nato Science, and the BMBF-Ministry of Research of Germany) for their support.

References

[1] C.F. von Weizsäcker, Die Atomkerne, Akademische Verlagsansstalt, Leipzig, 1937, pp. 40–52.
[2] S. Marsh, W.D. Rae, Phys. Lett. B 180 (1986) 185.
[3] J. Zhang, W.D.M. Rae, A.C. Merchant, Nucl. Phys. A 575 (1994) 61.
[4] H. Flocard, P.H. Heenen, S.J. Krieger, M.S. Weiss, Prog. Theor. Phys. 72 (1984) 1000.
[5] G. Leander, S.E. Larsson, Nucl. Phys. A 239 (1975).
[6] S. Aberg, L.O. Joensson, Z. Phys. A 349 (1994) 205.
[7] M. Freer, A.C. Merchant, J. Phys. G 23 (1997) 261.
[8] B.R. Fulton, W.D.M. Rae, J. Phys. G 16 (1990) 333;
B.R. Fulton, Z. Phys. A 349 (1994) 227 and refs. therein.
[9] K. Ikeda (Ed.), Proc. Fifth Int. Conf., Clustering Aspects in Nuclear and Subnuclear Systems, 1988, Kyoto, Japan, Phys. Society of Japan, 1989.
[10] W. von Oertzen, Z. Phys. A 354 (1996) 37;

W. von Oertzen, Z. Phys. A 357 (1997) 355;
also W. von Oertzen, Il Nuovo Cimento 110 A (1997) 895.
[11] K. Ikeda, N. Tagikawa, H. Horiuchi, Prog. Theor. Phys. Suppl. Extra Number (1968) 464.
[12] H. Horiuchi, K. Ikeda, Y. Suzuki, Prog. Theor. Phys. Suppl. 52 (1972), Chapter 3.
[13] W. von Oertzen, H.G. Bohlen, V. Subotin, Acta Phys. Polonica B 33 (2002) 93.
[14] Dao.T. Khoa, W. von Oertzen, H.G. Bohlen, Nucl. Phys. A 672 (2000) 387 and refs. therein.
[15] S. Ali, A.R. Bodmer, Nucl. Phys. 80 (1966) 99.
[16] D. Baye, Phys. Rev. Lett. 58 (1987) 2738.
[17] S. Ohkubo, et al., Prog. Theor. Phys. Suppl. 132 (1998) 1–133, in particular Chapter 2, F. Michel, S. Ohkubo, G. Reidemeister, pp. 7–72.
[18] W. von Oertzen, Eur. Phys. J. A 11 (2001) 403.
[19] H.G. Bohlen, et al., Prog. Part. Nucl. Phys. 42 (1999) 17.
[20] Y. Kanada-En'yo, H. Horiuchi, A. Ono, Phys. Rev. C 52 (1995);
also Y. Kanada-En'yo, H. Horiuchi, A. Ono, Phys. Rev. C 56 (1997) 1844.
[21] Y. Kanada-En'yo, H. Horiuchi, A. Dote, J. Phys. G 24 (1998) 1499;
Y. Kanada-En'yo, H. Horiuchi, A. Dote, Phys. Rev. C 60 (1999) 064304.
[22] Y. Kanada-En'yo, H. Horiuchi, Prog. Theor. Phys. 93 (1995) 115, and refs. therein.
[23] Y. Kanada-En'yo, H. Horiuchi, Phys. Rev. C 66 (2002) 024305, and refs. therein.
[24] A. Bohr, B. Mottelson, Nuclear Structure, Vol. II, Benjamin, Reading, MA, 1975.
[25] M. Milin, W. von Oertzen, Fizika (Zagreb), Memorial Volume for N. Cindro, 2003, in print.
[26] W. von Oertzen, Nucl. Phys. A 148 (1970) 529;
W. von Oertzen, H.G. Bohlen, Phys. Rep. C 19 (1975) 1.
[27] B. Imanishi, W. von Oertzen, Phys. Rep. 155 (1987) 29.
[28] N. Bischof, et al., Nucl. Phys. A 490 (1988) 490, and refs. therein.
[29] J.Y. Park, W. Greiner, W. Scheid, Phys. Rev. C 21 (1980) 958;
A. Thiel, J. Phys. G 16 (1990) 867–910.
[30] M. Brenner, T. Loennroth (Eds.), Proc. Int. Conf., Nuclear and Atomic Clusters, 1991, EPS Topical Conf., Turku, Finland, Springer, Berlin, 1992, p. 88.
[31] W. von Oertzen, Th. Wilpert, B. Bilwes, et al., Z. Phys. A 353 (1996) 373.
[32] I.P. Thompson, Comput. Phys. Reports 7 (1988) 167.
[33] J.M. Sparenberg, D. Baye, B. Imanishi, Phys. Rev. C 61 (2000) 054610.
[34] D. Scharnweber, W. Greiner, U. Mosel, Nucl. Phys. A 164 (1971) 257.
[35] G. Herzberg, Molecular Spectra and Molecular Structure, Vol. I, Spectra of Diatomic Molecules, van Nostrand, Princeton, 1950.
[36] F. Ajzenberg-Selove, Nucl. Phys. A 490 (1988) 1.
[37] S. Dixit, W. Bertozzi, T.N. Buti, et al., Phys. Rev. C 43 (1991) 1758.
[38] J.P. Glickman, W. Bertozzi, T.N. Buti, et al., Phys. Rev. C 43 (1991) 1740.
[39] H.G. Bohlen, et al., in: Yu.E. Penionzhkevich, E.A. Cherepanov (Eds.), Proc. Int. Symp., Exotic Nuclei, Lake Baikal, Russia, July 2001, World Scientific, Singapore, 2002, pp. 453–470.
[40] P. Descouvemont, Eur. Phys. J. A 12 (2001) 413.
[41] M. Freer, C. R. Physique 4 (2003).
[42] F. Ajzenberg-Selove, et al., Phys. Lett. B 40 (1972) 205.
[43] H.G. Bohlen, et al., Il Nouvo Cimento A 111 (1998) 841.
[44] H.G. Bohlen, et al., in: B. Rubio, et al. (Eds.), Proc. Int. Conf., Experimental Nuclear Physics in Europe, Sevilla, Spain, 1999, in: AIP Conf. Proc., Vol. 495, 1999, p. 303.
[45] H.G. Bohlen et al., submitted.
[46] P. Descouvemont, Nucl. Phys. A 699 (2002) 463.
[47] P. Descouvemont, D. Baye, Phys. Lett. B 505 (2001) 71.
[48] M. Freer, et al., Phys. Rev. Lett. 82 (1999) 1383.
[49] Y. Kanada-En'yo, Phys. Rev. C 66 (2002) 011303.
[50] N. Itagaki, et al., Phys. Rev. C 61 (2000) 044306.
[51] N. Itagaki, et al., Phys. Rev. C 64 (2001) 014301.
[52] M. Milin, W. von Oertzen, Eur. Phys. J. A 14 (2002) 295.
[53] W. von Oertzen, et al., 2003, to be published.